Theoretical study of collinear Be+FH(v_1)→BeF(v_2) +H[a)]

Heloiza Schor

Department of Chemistry, Columbia University, New York, New York 10027

Sally Chapman

Department of Chemistry, Barnard College, Columbia University, New York, New York 10027

Sheldon Green

NASA Institute for Space Studies, New York, New York 10025 and Department of Chemistry, Columbia University, New York, New York 10027

Richard N. Zare

Department of Chemistry, Stanford University, Stanford, California 94305
(Received 16 June 1978)

The potential energy surface for collinear Be+FH→BeF+H has been studied at various levels of *ab initio* approximation. A final surface was obtained from a first order configuration interaction wavefunction, using the iterative natural orbital method and a medium-sized basis set of Slater atomic functions; this is expected to give a semiquantitative description of the reactive process. The exothermicity is computed to be 6 kcal/mole which can be compared with the best experimental value of 2±4 kcal/mole. The barrier height is predicted to be 28 kcal/mole at a geometry where both internuclear separations are extended by about 0.4 bohr from their asymptotic equilibrium values. This surface differs qualitatively from simple LEPS models. The curvature of the reaction path is much more abrupt, the atom effecting little distortion of the partner molecule until quite close approach in both entrance and exit channels. The surface was fit with bicubic splines and dynamics was studied by the quasiclassical trajectory method as a function of initial kinetic energy for the reactant initially in $v_1 = 0$ and $v_1 = 1$. The reaction probability and final energy distributions were found to depend sensitively and selectively on the initial kinetic and vibrational energy. Most of the available energy is channeled into product translation; for $v_1 = 0$ at higher initital kinetic energies, less than 10% of the available energy becomes product vibration. Also, addition of reactant vibrational energy has a profound effect on reaction probability and final vibrational distributions. Examination of typical trajectories made it possible to identify the surface features responsible for the dynamical behavior. For comparison, calculations were also done on a LEPS surface constructed to have the same barrier position and height. Because the LEPS surface has a more gently curved reaction path, with better coupling of vibrational and translational energy, it results in less specific energy use and disposal. For example, 40%–50% of the available energy was channeled into product vibration on the LEPS surface, and addition of reactant vibrational energy effected only small changes in the dynamics. These results underline the dangers of using oversimplified potential surfaces in the study of reactive collision dynamics.

I. INTRODUCTION

A basic goal of chemical kinetics is to understand the details of reactive molecular collisions and, in particular, the way in which the shape of the electronic potential energy surface influences reactivity, energy specificity, and energy disposal. Experimentally, progress has been made in measuring reaction rates as a function of initial kinetic and internal energy and in analyzing the product in terms of translational, angular, and internal state distributions.[1] Theoretically, work has been done to obtain the same information via scattering calculations on electronic potential energy surfaces for reactive systems.[2] For a few systems the electronic surfaces were also computed *ab initio*. Because *ab initio* calculation of potential surfaces are generally expensive and must be repeated for each new system of interest, many of the scattering calculations to data have used (parameterized) model surfaces, such as the LEPS[3] model. In these latter studies it is easy to examine the manner in which variation of potential parameters affects collision dynamics. Such studies have been very useful for developing general rules which seem to explain the dynamics of some reactive systems. However, there is a danger that the model potentials in general use may not have sufficient flexibility to describe other systems and that rules based on these models may be misleading in some cases. In fact, the *ab initio* surface computed in this study differs significantly from model potentials in common use.

The motivation for the present study was recent experimental measurements of state-to-state rates for the reaction Ba + FH(v_1) → BaF(v_2) + H, where the reagent was initially in $v_1 = 0$ or $v_1 = 1$.[4] It was found that most of the available energy became product translational energy with very little channeled to product vibration. Similar results have been obtained recently for Sr and Ca reacting with FH.[5] This is contrary to predictions based on LEPS models, and Pruett and Zare[4] suggested that energy disposal in this system might reflect specific (non-LEPS) characteristics of the potential surface. Although *ab initio* calculation of the potential surface for this system would be quite expensive, it was

[a)]Supported by the National Aeronautics and Space Administration under Grant No. NSG 7105.

 0021-9606/78/6908-3790$01.00

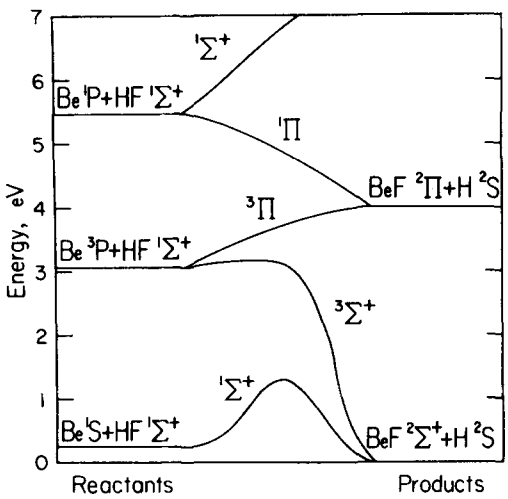

FIG. 1. Electronic correlation diagram for collinear BeFH. Note that 1 eV = 23.05 kcal/mole.

felt that the analogous Be + FH system, for which accurate *ab initio* calculations are feasible, might provide some insights. Because scattering calculations on *ab initio* potential surfaces have been performed for only a few systems to date, calculations for this system are of interest in their own right to extend our understanding of the shape of the potential surfaces for various types of reactive systems and its effect on collision dynamics. It is especially important to see whether such surfaces can, in general, be adequately represented by some of the models in current use.

The Be atom has an electronic ^1S ground state corresponding to a $1s^2 2s^2$ configuration; likewise the HF molecule has a closed-shell ground state electronic structure corresponding to $^1\Sigma^+ 1\sigma^2 2\sigma^2 3\sigma^2 1\pi^4$. The reaction is therefore expected to proceed on a singlet electronic surface, with overall $^1\Sigma^+$ symmetry for the collinear Be–FH approach. The products, which have open shell ground state electronic structures H^2S 1*s* and BeF $^2\Sigma^+ 1\sigma^2 2\sigma^2 3\sigma^2 4\sigma^2 5\sigma 1\pi^4$, also correlate with the $^1\Sigma^+$ BeF–H collinear surface. The products correlate with a (collinear) $^3\Sigma^+$ surface as well; but this is expected to be quite repulsive, analogous to the antibonding $^3\Sigma$ state of H_2, and to correlate with the excited Be ^3P $1s^2 2s2p$ electronic state of the reactants. Thus the reaction is expected to be described by nuclear motion on a *single* (ground state) electronic potential energy surface which is well separated from, and hence not influenced by excited electronic states (cf. Fig. 1). For such cases molecular collision dynamics should be adequately characterized by classical motion of the nuclei on this electronic potential energy surface.

We have obtained the ground state (collinear) electronic surface from theoretical calculations. A major concern in this study was to avoid biasing the results by preconceived models; hence calculations were performed at several levels of *ab initio* approximation. These calculations and the resulting potential surface are discussed in Sec. II. Collision dynamics on this surface were then studied with classical trajectories, and this is described in Sec. III; for comparison, analogous calculations on a LEPS model for this system are presented in Sec. IV. Findings are summarized in Sec. V.

II. ELECTRONIC POTENTIAL ENERGY SURFACE

Within the Born–Oppenheimer approximation, which is a fundamental assumption in this work, the potential energy surface is obtained by solving the electronic Schrödinger equation as a function of "clamped" nuclear positions. By using more and more elaborate wavefunctions it is possible to approach arbitrarily close to the true wavefunction and energy.[6] To describe a reactive surface, however, one needs the energy at a large number of nuclear positions—as will be seen, several hundred even for the relatively simple three atom collinear system considered here—so that an inexpensive level of approximation is desired. We have performed calculations at several levels of approximation to consider their adequacy for describing this system.

A. Hartree-Fock

Perhaps one of the most common approximations (and one which has been quite useful for many problems) is the single configuration or Hartree–Fock (HF) model. This method can be shown to give an "independent electron" description: Each electron moves independently in the field of the nuclei and the *average* field of the other electrons; instantaneous correlation of electron motions is ignored. Then the wavefunction is described by an antisymmetrized product of orbitals, and the variation principle determines the "best" orbitals. In practice the orbitals are expanded in a set of basis functions and the HF model leads to the best single configuration wavefunction within this basis. For a system the size of BeFH it is quite feasible to use expansions which approach the infinite (complete) basis set limit.

The HF approximation might be expected to be useful whenever a single configuration description is reasonable, and this is often the case. For example, in the Introduction the discussion of correlation between reactant and product electronic states was given in terms of the usual single configuration description of the low-lying atomic and molecular levels. However, a problem arises in the HF approach which, as we will see, makes it unsuitable for describing reactions such as the present one. If each orbital is allowed to vary freely in minimizing the energy (the unrestricted HF method) the resulting electronic function does not, in general, have the proper spatial and/or spin symmetry. To alleviate this, symmetry and equivalence restrictions are introduced; orbitals are allowed to vary only within certain constraints on their spatial and spin symmetry. Thus, the spatial symmetry of the nuclear framework is imposed: *s* and *p* functions for atoms, and σ and π functions for linear molecules. Also, electrons are paired with opposing spin functions in the same spatial orbital. The resulting *restricted* HF method, while often adequate to describe molecules near their equilibrium geometry, is generally inadequate to describe the breaking of bonds such as occurs in dissociation or reaction.

TABLE I. Comparison of molecular and reaction parameters obtained from different theoretical calculations and from experiment.

	Hartree-Fock				Configuration interaction				Expermment
Basis set[a]	I	II	IV	limit[b]	I	II	III	IV	
Re(FH), a.u.	1.93	1.93	1.84	1.70[c]	2.05	2.05	2.00	1.88	1.73[d]
De(FH), kcal/mole	38	38	50	101[c]	60	60	63	100.6	138.3 ± 1.0[e] 141.3 ± 0.5[f]
Re(BeF), a.u.	unb.[g]	unb.	2.61	2.56	unb.	unb.	2.94	2.60	2.57[d]
De(BeF), kcal/mole	unb.	unb.	87	116	unb.	unb.	29	106.5	138.8 ± 4[h]
ΔE, kcal/mole	•••	•••	−37	−15	•••	•••	+34	−5.9	0.4 ± 4 −2.5 ± 4
Barrier:									
E, kcal/mole	•••	•••	•••	•••	•••	•••	•••	28	•••
R_{FH}, a.u.	•••	•••	•••	•••	•••	•••	•••	2.35	•••
R_{BeF}, a.u.	•••	•••	•••	•••	•••	•••	•••	3.00	•••

[a]The basis sets are given in Table II and discussed in the text.
[b]Large basis sets thought to approach the infinite basis set limit.
[c]P. E. Cade and W. M. Huo, J. Chem. Phys. **47**, 614 (1967).
[d]B. Rosen, *Donnêes Spectroscopiques* (Pergamon, Oxford, 1970).
[e]V. H. Dibeler, J. A. Walker, and K. E. Mcculloh, J. Chem. Phys. **51**, 4230 (1969).
[f]W. A. Chupka and J. Berkowitz, J. Chem. Phys. **54**, 5126 (1971).
[g]Unb. indicates that molecule was not bound at this level of approximation.
[h]T. E. H. Walker and R. F. Barrow, J. Phys. B **2**, 102 (1967).

This problem can be illustrated by again considering the correlation of reactants and products here. The reactants, Be + HF, are described by the closed-shell configuration $1\sigma^2 2\sigma^2 3\sigma^2 4\sigma^2 5\sigma^2 1\pi^4$ where, in collinear geometry the Be s orbitals become σ orbitals. The products, BeF + H, on the other hand, must be described as $1\sigma^2 2\sigma^2 3\sigma^2 4\sigma^2 5\sigma 6\sigma 1\pi^4$; here one of the unpaired σ electrons corresponds to H 1s and the other to the unpaired BeF electron. The products cannot be described as a closed-shell configuration in the restricted HF approximation since then the paired (singlet coupled) electrons would be forced to share the same spatial orbital. Therefore, while the HF method might provide an adequate asymptotic description of both reactants and products, it cannot describe the continuous deformation along the reaction path.

Because the Hartree–Fock method is in standard use for many electron structure applications we have considered its utility further. As noted, by employing different orbital configurations, we can separately describe the reactants and products, and the Hartree–Fock values for some relevant (asymptotic) reaction parameters obtained by this method are shown in Table I. Starting from the asymptotic Hartree–Fock solutions, it is possible to do calculations into the reactive region. At some point the energies obtained this way will cross as the reagent configuration goes to excited states of the product and *vice versa*. It was thought that it might be possible to get an idea of the barrier position and height by starting from both ends and looking for this crossing; however, this occured at such a high energy that it did not seem to provide any useful information.

B. Configuration interaction

It is apparent that reactive potential surfaces will, in general, need a multiconfiguration description. The problem is then twofold: choosing the configurations and choosing the orbitals. These are interrelated since a poor choice of orbitals will lead to slow convergence of the CI wavefunction as configurations are added. Thus, the Hartree–Fock orbitals for the closed-shell (reactant-like) configuration will provide a poor basis for describing the open-shell products and *vice versa*.

If all possible N-electron configurations that can be constructed from a (finite) set of orbitals are included in the CI wavefunction, it is invariant to a unitary transformation among the orbitals. That is, if one constructs a *complete* CI, the choice of orbitals is immaterial. The complete CI is an attractive method for reactive surfaces insofar as it provides an unbiased description (within the limits of the expansion basis, of course) of changes in bonding, e.g., bond breaking, bond formation, charge transfer, etc. The drawback of this method is that the number of possible configurations grows extremely rapidly as the number of basis functions is increased, and applications have generally been limited to minimum basis set calculations, i.e., one basis function for each occupied orbital in the separated atoms.

We have performed minimum basis set full CI calculations for this system. The Slater-type basis included one function for each atomic orbital (H 1s, Be 1s2s, and F 1s 2s2p) with the orbital exponents obtained by optimizing the Hartree–Fock energies of the

TABLE II. Basis sets of Slater-type (screened exponential) orbitals used in the present study. Basis I is the usual minimum basis set. Basis II has, in addition a Be $2p\sigma$ function. Basis III was obtained by optimizing the orbital exponents of Basis II for the molecular environment. Basis IV was used in the final calculations.

		Basis I[a]	Basis II	Basis III	Basis IV
Be	1s	3.6848	3.6848	3.6893	3.73315
Be	2s	0.9560	0.9560	1.0576	1.03781
Be	2s	•••	•••	•••	1.61052
Be	$2p\sigma$	•••	1.1278	1.2650	1.25864
Be	$2p\pi$	•••	•••	•••	1.22427
F	1s	8.6501	8.6501	8.6501	8.64472
F	2s	2.5638	2.5638	2.51383	2.63255
F	2s	•••	•••	•••	1.01188
F	$2p\sigma$	2.5500	2.5500	2.43658	4.13710
F	$2p\sigma$	•••	•••	•••	1.93090
F	$2p\pi$	2.5500	2.5500	2.4345	1.81506
F	$2p\pi$	•••	•••	•••	4.29163
H	1s	1.0000	1.0000	1.0000	1.00000

[a]E. Clementi and D. L. Raimondi, J. Chem. Phys. **38**, 2686 (1963).

separated atoms; these are listed in Table II. With this basis one can build 22 configurations of $^1\Sigma^+$ symmetry. Unfortunately, test calculations showed the inadequacy of this level of approximation for the system under study. In particular, it predicts no bonding in the BeF product molecule (cf. Table I).

An apparent inadequacy of the minimum basis set is lack of a Be $2p$ function. It is well known that this is important in describing atomic Be since the $2s$ and $2p$ orbitals are nearly degenerate in energy. Addition of a Be $2p\sigma$ function is expected to improve the description of the BeF bond by allowing for sp hydridization. Accordingly, we increased the minimum basis by adding a Be $2p\sigma$ function with exponent $\zeta = 1.1278$. Addition of this single orbital increases the number of possible $^1\Sigma^+$ configurations to 225. However, test calculations with this basis at both the Hartree–Fock and CI level (including the most important 200 configurations) indicated that it was still inadequate to predict a bound BeF product (cf. Table I).

The basis set still contains some flexibility without the necessity of adding more functions in that it is possible to reoptimize the Slater orbital exponents to better describe the molecular environment. As a general rule of thumb it has been found more economical to use a larger number of functions rather than to reoptimize a smaller basis set. Nonetheless, some limited optimization was tried to see whether an adequate description could be obtained this way. Although this provided some improvement, it appeared that such a small basis simply does not have adequate flexibility to give a good description along the reaction path.

Having found it necessary to use a larger set of basis functions, it is no longer feasible to include all possible configurations. It is then necessary to choose the orbitals and configurations in an optimal way. It can be shown that a specific set of orbitals provides the most rapid convergence (in a certain sense) of the CI calculation as a function of the number of configurations included. These are the so-called natural orbitals.[7] Unfortunately, to obtain these requires a knowledge of the exact wavefunction, since they are the orbitals which diagonalize the first order density matrix of the exact wavefunction. It is possible, however, to obtain approximate natural orbitals. For example, in the iterative natural orbital scheme introduced by Bender and Davidson,[8] one obtains "approximate" natural orbitals which diagonalize the first order density matrix of some trial CI function; these are used to generate a second CI wavefunction which gives a new set of approximate natural orbitals; and this process is iterated. Note that there is generally no guarantee of "convergence" in this iterative scheme, but it has been found to be effective in a number of studies.

There still remains the choice of which configurations to include in the CI wavefunction. Of the many schemes that have been tried or suggested, the "first order wavefunction" as developed by Schaefer and co-workers[9] seems particularly attractive for the current study for several reasons. First, this method includes in a systematic way the configurations needed to describe the breaking and formation of bonds. Second, it leads to a relatively small number of configurations. Finally, a CI wavefunction with configurations chosen according to this scheme is well suited for use in conjunction with the iterative natural orbital method to optimize the description of the orbitals.

The first order wavefunction includes all configurations which differ little in energy from the Hartree–Fock configuration (i.e., all excitations within the valence shell) and the first order correction of deficiencies associated with double orbital occupancy (configurations where at most one electron is excited beyond the valence shell). The definition of "valence" shell can be interpreted loosely if necessary to include important effects; in particular, the Be $2p$ orbital, as noted previously, is important for describing correlation in this system although it might rigorously be excluded from the valence orbitals. To keep the configuration list at a reasonable length it is common to restrict excitations among the valence shell so that only certain kinds of single and double excitations from the ground state configuration are included. Since there are two important ground state configurations here, one for reactants and one for products, we have included the same kind of excitations from both of these reference configurations. Also, the lowest two orbitals were kept doubly occupied in all configurations since these correspond to F $1s$ and Be $1s$ core electrons which are expected to remain essentially unchanged over the potential surface. The final CI wavefunction included 198 configurations of $^1\Sigma^+$ symmetry; these are given in Table III.

The basis set used in the first order CI calculation was somewhat more flexible than the minimum basis set (cf. Table II). However, a single function was still used to describe the core F $1s$ and Be $1s$ orbitals. To improve the quality of this limited basis set, some optimization of the orbital exponents was done for a few

TABLE III. Configurations included in the first order wavefunction.

Reference configurations			
I	$1\sigma^2 2\sigma^2 3\sigma^2 4\sigma^2 5\sigma^2 1\pi^4$		
II	$1\sigma^2 2\sigma^2 3\sigma^2 4\sigma^2 5\sigma 6\sigma 1\pi^4$		
Single excitations			
I	$n\sigma \rightarrow m\sigma$,	$n = 3-5$,	$m = 7-10$
II	$n\sigma \rightarrow m\sigma$,	$n = 3, 4$,	$m = 5-10$
II	$5\sigma \rightarrow m\sigma$,	$m = 6-10$	
I, II	$2\sigma \rightarrow m\sigma$,	$m = 6, 7$	
I, II	$1\pi \rightarrow m\pi$,	$m = 2, 3$	
Double excitations			
I	$n\sigma^2 \rightarrow m\sigma^2$,	$n = 3, 4$,	$m = 6, 7$
I	$5\sigma^2 \rightarrow 7\sigma^2$		
II	$n\sigma^2 \rightarrow 7\sigma^2$,	$n = 3, 4$	
I, II	$n\sigma 5\sigma \rightarrow 7\sigma^2$,	$n = 3, 4$	
I	$3\sigma 4\sigma \rightarrow m\sigma^2$,	$m = 6, 7$	
II	$3\sigma 4\sigma \rightarrow 7\sigma^2$		
I, II	$n\sigma^2 \rightarrow 6\sigma m\sigma$,	$n = 3, 4$,	$m = 7-10$
I	$n\sigma^2 \rightarrow 7\sigma m\sigma$,	$n = 3-5$,	$m = 8-10$
II	$n\sigma^2 \rightarrow 7\sigma m\sigma$,	$n = 3, 4$,	$m = 8-10$
I, II	$3\sigma 4\sigma \rightarrow 6\sigma m\sigma$,	$m = 7-10$	
I, II	$3\sigma 4\sigma \rightarrow 7\sigma m\sigma$,	$m = 8-10$	
I, II	$n\sigma 5\sigma \rightarrow 7\sigma m\sigma$,	$n = 3, 4$,	$m = 8-10$
II	$n\sigma 5\sigma \rightarrow 6\sigma m\sigma$,	$n = 3, 4$,	$m = 7-10$
I	$1\pi 1\bar{\pi} \rightarrow 2\pi m\bar{\pi}$,	$m = 2, 3$	
II	$1\pi 1\bar{\pi} \rightarrow 2\pi 3\bar{\pi}$		
I	$1\pi 1\bar{\pi} \rightarrow m\sigma^2$,	$m = 6, 7$	
II	$1\pi 1\bar{\pi} \rightarrow 7\sigma^2$		
I, II	$1\pi 1\bar{\pi} \rightarrow 7\sigma m\sigma$,	$m = 8-10$	
II	$1\pi 1\bar{\pi} \rightarrow m\sigma m'\sigma$,	$m = 5, 6$,	$m' = 7-10$

geometries. This basis (Basis IV in Table II) is still far from the Hartree–Fock limit, and is not expected to give quantitative accuracy. Nonetheless it is believed to be a reasonable compromise between accuracy and economy. It should be flexible enough to describe the important changes in bonding in this reactive system; it is expected to give a reasonable representation of the shape of the potential energy surface.

Calculations were done for a large number of geometries to map the potential as a function of the BeF and FH distances. The former was varied from 2.1–10.0 bohr and the latter from 1.3–10.0 bohr. The smaller distances are well inside the classically forbidden region, and the interaction is negligible at the larger distances. The final potential is shown as a contour plot in Fig. 2, and some relevant properties are summarized in Table I.

The final potential energy surface which is displayed in Fig. 2 shows several interesting features and differs considerably from simple model surfaces in common use; these points will be considered in detail below in connection with the scattering calculations. It seems appropriate here to comment on the expected accuracy of this surface and to summarize our experience with the various levels of approximation. The only way to quantitatively judge the accuracy of the present calculation would be to perform larger calculations. We have not done this, partly because of expense and partly because it is felt that the present results provide a realistic description. The major shortcoming in the present work is the limited basis set. The first order configuration interaction method is thought to include all important effects; if other types of configurations were important it would have been apparent in the smaller basis full CI calculations. Within the first order CI method, it is somewhat inconvenient to increase the basis set size since that also increases the number of configurations. In this context it should be noted that two others methods, the multi configuration SCF[10] and the generalized valence bond[11] approach, provide a similarly good description of changes in bonding along a reactive surface and should be more readily capable of employing larger basis sets. Such calculations were not pursued in the present study, but it is expected that they will be quite useful in future work. In summary, it is apparent that a multiconfiguration description will generally be necessary for studying reactive surfaces, and that a reasonably large basis set, capable of describing at least both the reactants and the products, must be used. The first order CI calculation presented here is probably the minimum needed to obtain an adequate semiquantitative description.

C. Fitting the surface

The result of an *ab initio* calculation is a set of numbers which represents the potential $V(R_{HF}, R_{BeF})$ at dis-

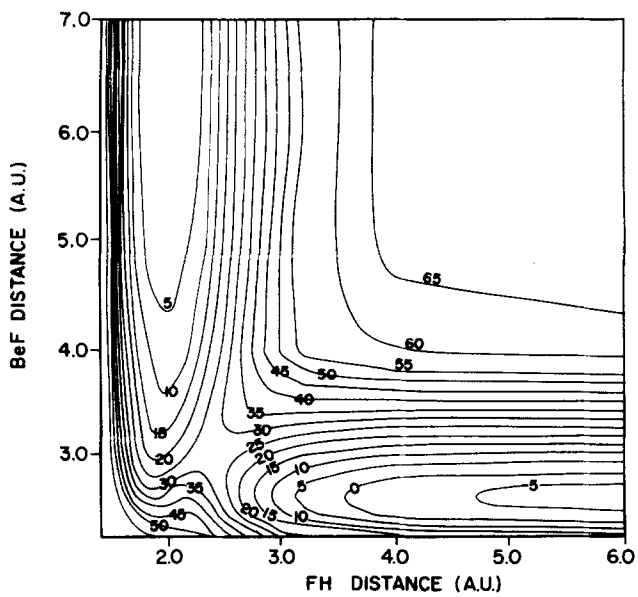

FIG. 2. Potential energy contours for collinear BeFH obtained from an *ab initio* (first order configuration interaction) calculation. Distances are in atomic units (1 a.u. = 0.52918×10^{-8} cm); contour units are kcal/mole.

crete points. In order to perform dynamical calculations it is necessary to have a continuous representation of the potential. For classical trajectory calculations it is imperative that this representation have continuous first derivatives as well. There are basically two approaches that can be used to obtain a continuous potential: a global fit to the computed points or an interpolation procedure which is essentially a local fit. In the former, one fits the entire surface to some functional form; in the latter, different functions are used for different parts of the surface.

Many of the global fitting procedures attempt to choose a functional form based on simple models of molecular bonding. Among these are the frequently used LEPS model and the more recent diatomics-in-molecules[12] (DIM) method. By building a certain amount of physics into the functional form, it is hoped that the surface can be characterized by relatively few parameters so that knowledge of the potential at only a few points is required. Since the asymptotic (reactant and product) potentials are usually well known, global fits generally build the correct asymptotic behavior into the functional form. These advantages of the global approach, however, are also its weaknesses: the assumed functional form severely constrains the flexibility. Thus, parameters in these models are usually chosen to fit certain features of the surface which are thought to be important, such as barrier position and height, but this constrains the potential in other regions of configuration space which may (or may not) be important for describing collision dynamics. It would appear that our current state of knowledge concerning the relative importance of different aspects of the surface makes it unwise to use functional forms that are more restrictive than necessary.[13]

We have made some attempt to fit the calculated BeFH surface to a LEPS model with three adjustable parameters (cf. Sec. IV). Although the asymptotic regions could be accurately reproduced, it did not seem possible to obtain a good fit in the region of strong interaction using such an inflexible function. The *ab initio* calculations were done on a nonuniform grid with many more points in the region of strong interaction; much of this information is lost in a global fit in exchange, perhaps, for some extra precision in regions where few points were calculated.

It is, of course, possible to obtain an arbitrarily accurate global fit to a complicated surface by (Fourier) expanding in some complete set of functions, the most familiar example, perhaps, being Taylor expansion in polynomials. The problem here is that an accurate fit generally requires many terms and hence many parameters. Such a complicated function retains little of the physical insight into the nature of the surface which is an asset of simple, modelistic functional forms. Furthermore, it becomes computationally expensive to evaluate. Such an approach seems to have little to recommend it.

Interpolation is based on obtaining local fits. By limiting the region of validity, it is possible to obtain good accuracy with a simple, but general functional expansion, most commonly a low order polynomial. Interpolation schemes are particularly well suited to take advantage of a nonuniform grid, with more values in regions of rapid variation, as is commonly the case in *ab initio* calculations of potential surfaces. Of various available interpolation schemes, cubic splines[14] offer certain advantages for classical trajectory calculations, for example, continuous first derivatives. Several classical trajectory studies have indicated the utility of cubic spline interpolation.

For the two-dimensional collinear surface here, interpolation was done with a two-dimensional spline. This is a bicubic polynomial piecewise defined by $S(x_n, y_m)$ on the rectangle given by the nodes (x_n, x_{n+1}), (y_m, y_{m+1}). The coefficients of the polynomial in each rectangle are determined by requiring several conditions: (1) the polynomials pass through the node points, which ensures a continuous function, (2) the first and second partial derivatives are continuous at the nodes,, which ensures a smooth function, and (3) the second partial derivatives vanish at the end nodes, which gives the so-called "natural" spline. In the present study, this interpolation was accomplished with routines available from standard computer program libraries.[15]

Some problems were encountered in effecting the spline fit and it seems worthwhile to discuss these. The accuracy of the fit was found to be sensitive to the distance between nodes. In particular, in regions where the potential is flat, such as the asymptotic entrance and exit valleys, the spline tends to give oscillatory behavior when the distance between nodes is too great. This was corrected by calculating or estimating the potential at additional grid points. The fit was considered adequate when additional grid points no longer had a significant effect on typical trajectories. Although it might be assumed that trajectories are insensitive to the potential in classically forbidden regions, for example, in the three atom dissociative region, it was found that these regions did, in fact, influence the fit through constraints on the continuity of derivatives. In the asymptotic regions, and especially in the three atom region, it was generally adequate to generate additional points by linear interpolation; at short distances extrapolation was done by fitting an exponential form.

In classical trajectory calculations, numerical accuracy depends strongly on the smoothness of derivatives of the interaction. Therefore, we also experimented with fitting splines directly to values of the potential derivatives which were obtained from the potential in regions where the fit was not problemmatic. This procedure suggested itself when it was observed that the derivative in the initial spline fit sometimes showed oscillatory behavior even where the function appeared reasonably smooth. While this proved to be an effective method, it seemed more cumbersome than necessary.

III. CLASSICAL TRAJECTORY CALCULATIONS

The classical trajectory method has been used extensively in studies of the dynamics of molecular collisions in reactive systems. Studies on model systems have given insight into the relationship between potential surface features and reaction dynamics.[3] Good agreement with experiment has been found in trajectory studies on potential energy surfaces which have been verified by *ab initio* calculations.[16] Finally, the results of quantum

dynamical calculations have been compared with classical trajectories on the same surface both for collinear and three dimensional collisions.[17] These studies indicate that, in general, classical results are useful in an averaged sense: Quantum dynamics gives rise to oscillatory structure which is absent in the corresponding classical result, but the classical calculation usually gives the appropriate underlying shape. In three dimensions averaging over orientation reduces the interference structure considerably, so that the comparison between quantum and classical dynamics improves. Thus with some confidence we believe that classical trajectories will provide an adequate picture of the dynamics on this potential energy surface.

A. Numerical methods

The classical trajectories were generated using standard methods.[18] The two coordinates, R and r were defined such that R is the distance from the atom to the center of mass of the molecule for the initial arrangement, and r is the length of the molecule. These coordinates give rise to a particularly simple Hamiltonian:

$$H = P^2/2\mu + p^2/2m + V(R, r),$$

where P and p are the momenta conjugate to R and r, respectively, and μ and m are the appropriate reduced masses. The initial conditions were selected so that the atom and moleucle are sufficiently separated that their interaction is negligible, the relative translational energy E_T is fixed, and the vibrational energy E_V is that of an HF molecule in the specified state. It is this quantization of the diatomic energy which suggests the term "quasiclassical trajectories."

One additional parameter is required to complete the initial conditions: the vibrational phase, ϕ. This was varied within a batch of trajectories. The particular choice for each trajectory can be made in any one of several ways. In three dimensional triatomic collisions where there are five or more parameters to be varied, it is customary to use Monte Carlo sampling techniques, although other approaches have been suggested.[19] However, for collinear collisions with just a single parameter, systematic sampling methods are expected to give better precision for the same number of trajectories. Thus, with exceptions noted below, ϕ was selected uniformly between 0 and 2π. If the asymptotic molecule can be described by a harmonic oscillator or by a Morse curve it is possible to use action angle variables to relate the phase to the coordinate and momentum r and p.[20] Because the surface we are using is not analytic, we have adopted a slightly different approach. The vibrational state v_1 was obtained from spectroscopic data. The vibrational turning points r_+ and r_- and the period τ for that energy were obtained numerically. When an initial phase was selected, the diatomic was placed at r_+ if $\phi < \pi$, and r_- if $\phi > \pi$. At this point $p = 0$. A two body integration was carried out for a time interval $t = \phi(\mathrm{mod}\pi)/2\pi$. At this point, the collision began.

The four canonical equations of motion were integrated using a fourth order predictor–corrector algorithm with continuously variable step size.[21] The potential and first derivatives were obtained from the bicubic spline fit to the *ab initio* surface points as discussed in Sec. II.C. The error criterion in the integration was established so that energy conservation was always better than 7×10^{-5} kcal/mole.

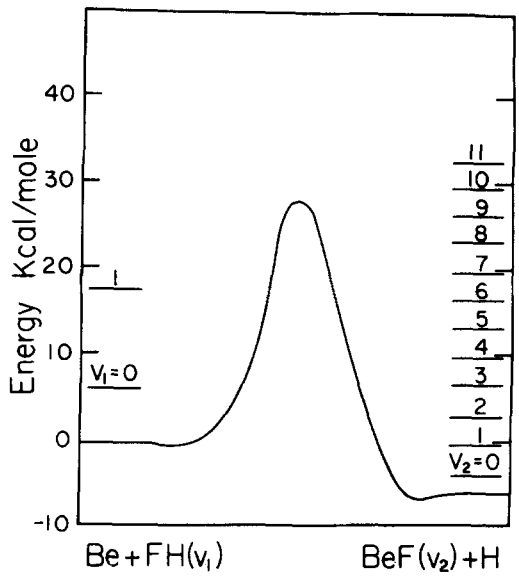

FIG. 3. Schematic diagram of energy quantities involved in the reaction Be + FH(v_1) → BeF(v_2) + H. The exothermicity and barrier height are those obtained from an *ab initio* calculation.

The total reaction probability $P_R(E)$ was calculated as the fraction of the trajectories which react. Improved precision for this quantity can be obtained with a small number of additional trajectories by making use of the fact that there are broad bands of reactive and nonreactive trajectories as a function of ϕ, so that one need define only the band edges with precision.[22] The edges of the bands are not always distinct, sometimes characterized by regions where the outcome varies rapidly with phase. This region has been termed the "statistical region,"[20] and is related to complex collision events. For the Be + FH reaction, the statistical region was never more than 2% of the total range of ϕ.

The distribution of vibrational energy in products has been calculated in terms of a quantity $P(v_1, v_2)$, the probability that a reactive trajectory initiating in state v_1 reaches product state v_2. $P(v_1, v_2)$ was determined by the usual histogram method: v_2 was the quantum number whose energy was closest to the classical product vibrational energy. Over at least 95% of the range of ϕ the final vibrational energy is a simple smooth function so that improved precision in the result can be obtained as above by using small additional samples of trajectories to define the boundaries between successive values of v_2 with greater accuracy.

B. Results

Various energy quantities play a central role in any discussion of collision dynamics: exothermicity, barrier height, vibrational energy, etc. For convenience, the energetic quantities for this system are shown schematically in Fig. 3. The total reaction probabilities as a

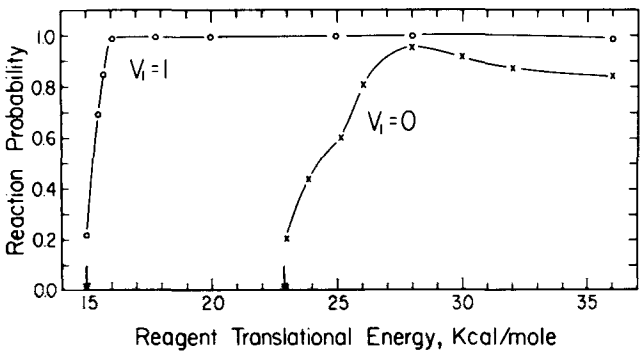

FIG. 4. Reaction probability as a function of initial kinetic energy for Be + FH(v_1) → BeF + H, $v_1 = 0$ and $v_1 = 1$, obtained from collinear classical trajectory calculations on an *ab initio* potential surface. Arrows on the abscissa indicate threshold energies

function of translational energy for Be + FH($v_1 = 0$) and ($v_1 = 1$) are shown in Fig. 4. Clearly the effects of energy in this system are specific: The extra vibrational energy results in a qualitatively different curve. The added vibrational energy results in less translational energy being required to surmount the barrier, but the effect is not additive: The total energy at threshold has increased. More important is the difference in shape of the two $P_R(E)$ functions. For Be + FH($v_1 = 0$) the function rises slowly from threshold, never reaches unit probability, and falls gently from a maximum about 5 kcal/mole above threshold. For vibrationally excited reactants, the function rises steeply from threshold reaching unit probability within 1 kcal/mole and continues at unit probability over a wide energy range.

The reaction probability distributed over product vibrational states, $P(v_1, v_2)$, shows more dramatically the specific nature of this reaction. Histograms for selected energies are shown in Fig. 5. (Complete results are given in Ref. 23). The distributions are shown at four characteristic energies for both vibrationally cold and vibrationally excited reactants: at threshold, slightly above threshold where the total reaction probability is still rising, at 28, and at 36 kcal/mole.

For vibrationally cold reactants the distributions show a strong energy dependence. At threshold the disposition of energy is very specific, with $v_2 = 3$ strongly preferred. As the translational energy increases the distribution spreads and lower product states begin to be populated. At a translational energy such that the total reaction probability has reached its maximum, the product state distribution falls monotonically from $v_2 = 0$. As the initial translational energy increases, so increases the fraction of translational energy in the products. It should be noted that even near threshold there is sufficient energy to populate BeF to $v_2 = 10$ (cf. Fig. 3) so that these distributions reflect a strong preference for product translation.

For vibrationally excited FH the picture is quite different. The additional reactant vibrational energy results in significantly greater product vibration. The distributions have a qualitatively different shape: They are broader, and they peak towards the largest v_2 populated. The translational energy dependence differs also: The trend is more gradual and the distributions become less sharp as energy increases. Another measure of energy partitioning is shown in Fig. 6. Shown is the fraction of energy in product vibration. For both $v_1 = 0$ and $v_1 = 1$ the fraction is greatest at threshold, and falls to an approximately constant value at high energy.

C. Relation of dynamics to potential surface

An appealing aspect of collinear reactive studies is that the low dimensionality facilitates a detailed examination of the influence of the potential on collision dynamics. Thus, for a given initial vibrational level and kinetic energy, the collision depends on only a single variable, the initial vibrational phase. As might be expected, small changes in the initial vibrational phase generally cause relatively smooth changes in collision

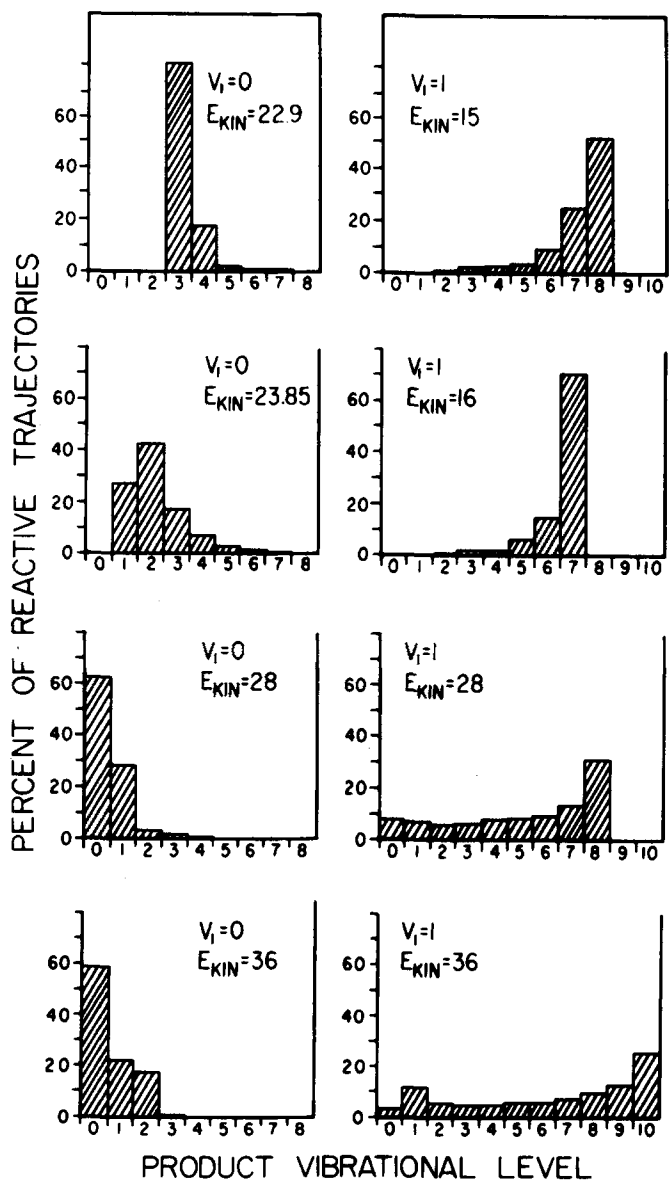

FIG. 5. Distribution among product vibrational levels for Be + FH → BeF + H for selected initial translational energies (in kcal/mole) and initial vibrational levels $v_1 = 0$ and $v_1 = 1$. Results were obtained from collinear classical trajectory calculations on an *ab initio* potential surface.

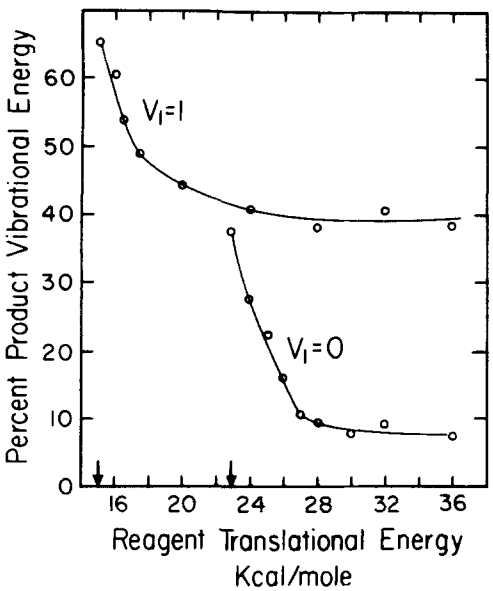

FIG. 6. Percent of available energy in product vibration for Be + FH(v_1) → BeF + H, $v_1 = 0$ and $v_1 = 1$, as a function of initial translational energy. Results were obtained from collinear classical trajectory calculations on an *ab initio* potential surface. Arrows on the abscissa indicate threshold energies. Solid lines have been drawn through the computed points as an aid to visualization.

dynamics, although more complicated behavior is sometimes observed. It has proved useful in other systems to consider the behavior of dynamics as a function of the initial vibrational phase, and we present here such an analysis of our results. Where the behavior with vibrational phase is well behaved, it is expected that trajectories are sampling similar regions of the potential surface. We then consider a number of trajectories which illustrate in detail how the dynamics in this system are influenced by specific features of the potential energy surface.

Figure 7 shows the final vibrational energy as a function of the phase ϕ for selected translational energies for Be + FH($v_1 = 0$). Keeping in mind that the absolute value of ϕ is arbitrary, one sees a fairly steady trend. Near threshold the curve is smooth and simple. As energy increases, the curve broadens reflecting increased reactivity, but it begins to become more complicated in shape. At the highest energy shown there are regions in which the product vibrational energy is a seemingly discontinuous function of the initial phase, although most of the range has smooth segments. The boundaries between reactive and unreactive areas are quite sharp, in contrast to observations on some other systems.[20]

Figure 8 shows analogous curves for the Be + FH($v_1 = 1$) reactions. The sharp contrast is evident. It is interesting to note that, while the system reacts with unit probability over a range of energies, there is a persistent discontinuity in the curve and a surrounding range where the product vibrational energy is a very steep function of the initial phase. The domain of this apparent discontinuity is narrow, but it is evident that it is into this gap that the unreactive trajectories begin to occur at high energy.

Another way of representing these results is to map the regions of reactive and unreactive trajectories in the (E_{trans}, ϕ) plane. Similar studies of H + H_2[22,24] have lent insight into the relationship between surface and dynamics. Maps of these reactive bands for Be + FH($v_1 = 0$) and Be + FH($v_1 = 1$) are shown in Fig. 9. Previous observations are underscored: First, there is a fairly simple continuity in the reactive bands, and second, additional vibrational energy results in a qualitatively different outcome. An interesting new feature can be observed: The failure of the Be + FH($v_1 = 0$) to reach unit probability is evidenced by a persistent unreactive band which extends to almost 36 kcal/mole translational energy. However, there is a new and quite distinct unreactive band which first appears at about 35 kcal/mole. This possibly suggests a common mechanism for high energy unreactive events.

We turn now to consider in some detail how the dynamics are affected by specific aspects of the potential energy surface. This system is characterized by a rather sharp change in electronic configuration between the entrance Be + FH and the exit BeF + H channels. This results in a substantially different appearance of this surface as compared with the well studied H + H_2 [25] or F + H_2 [26] systems. The reaction path in the entrance channel rises in energy as the reactants approach, but there is little curvature—little distortion of the FH equilibrium geometry from its asymptotic value. After an ascent of about 15 to 20 kcal/mole, the barrier appears suddenly at an extended Be–F and F–H geometry. The reaction path (the path which falls by steepest descent from the top of the barrier) curves sharply over the top of the barrier rising another 10 to 15 kcal/mole, and is oriented at the saddle point nearly along the initial vibrational coordinate. The sharp change in electronic configuration results in a fairly narrow pass between reactants and products, with a rather pronounced shoulder extending towards the saddle point from the repulsive wall.

While the coordinates of Fig. 2 and of the trajectories shown below are simply the bond lengths R_{BeF} and R_{FH}, it should be noted that, because it is a relatively heavy particle which is being transferred, the transformation that would diagonalize the kinetic energy with a single effective mass would cause little significant distortion: the abscissa would scale by a factor of 0.48, but the angle would remain about 90°.

A reactive trajectory at the threshold for the Be + FH ($v_1 = 0$) reaction is shown in Fig. 10. The reactants enter at the top of the figure. Translation and vibration are initially poorly coupled: The envelope to the vibrational amplitude is virtually constant until very close approach, while the translational energy is drained as the intermolecular potential rises. The trajectory is quite suddenly deflected into the product valley. The total energy of the system is sufficiently low that the trajectory passes very close to the saddle point, with little excess kinetic energy. Because the BeF separation at the col is extended, and because the product valley, like the

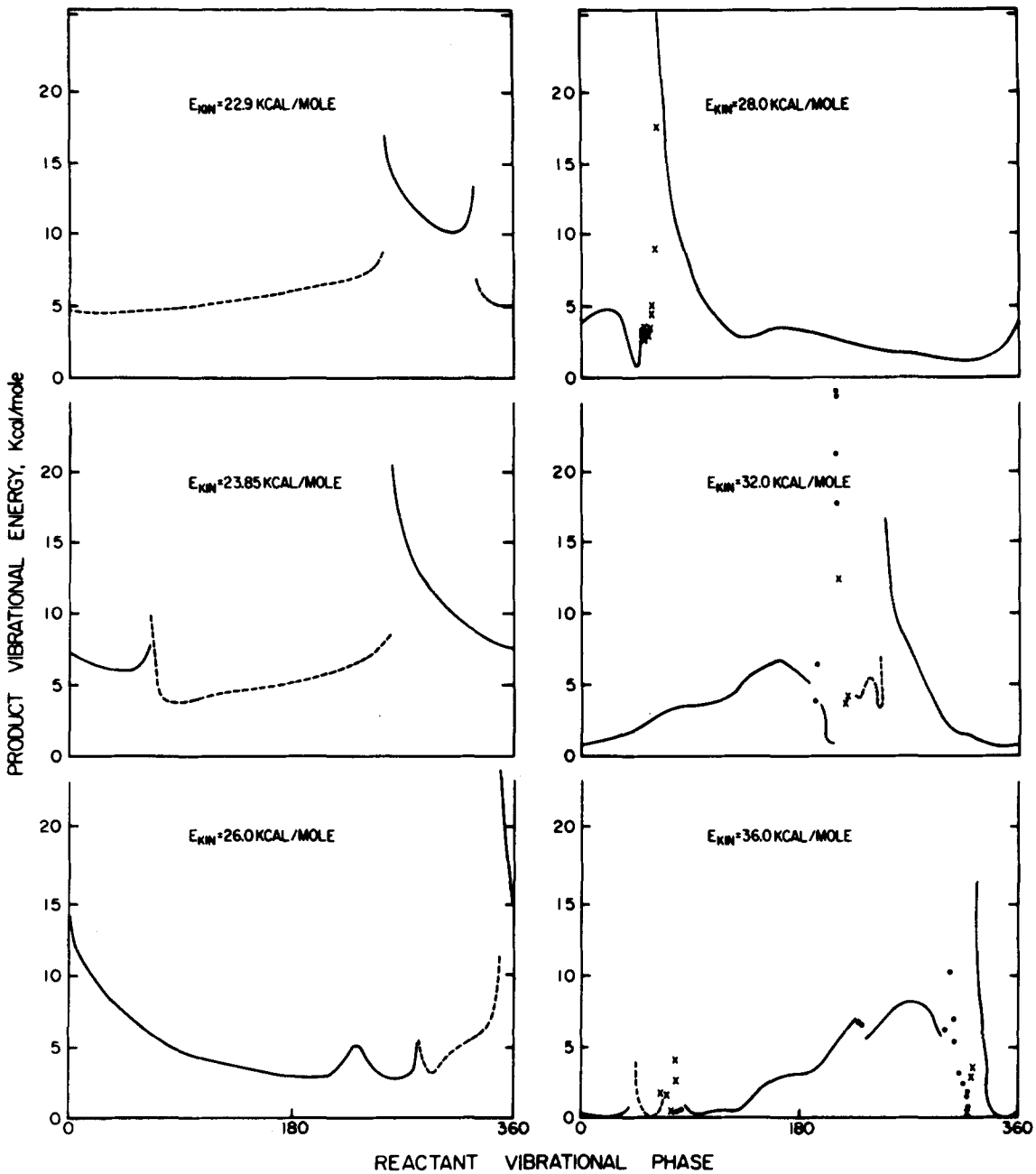

FIG. 7. Final energy in vibrational motion for Be + FH collisions at selected initial translational energies as a function of the initial FH vibrational phase. The FH molecule was initially in its $v_1 = 0$ vibrational level. Results were obtained from collinear classical trajectory calculations on an *ab initio* potential surface. For reactive trajectories the energy in product BeF vibration is shown as a solid line, or, where the product vibrational energy is varying rapidly as a function of initial phase, as dots. For nonreactive trajectories, the energy remaining in FH vibration is shown as a broken line, or by crosses.

reactant valley, shows little curvature and couples vibration and translation only very weakly, the product molecule has considerable vibrational excitation.

As the translational energy increases, the width of the pass which is energetically accessible increases, but as is shown in Fig. 11 a successful reaction still in general requires a deflection of the trajectory at a small Be–F distance in order to channel energy into the direction needed to surmount the barrier. Thus while P_R increases with energy, there remains a range of initial phases which give rise to unreactive collisions.

This behavior is in sharp contrast to the Be + FH($v_1 = 1$) collisions. A threshold trajectory for this system is shown in Fig. 12. Again, coupling of translational and vibrational energy in the entrance valley is poor. However, in this case the amplitude of the FH vibration is sufficient to carry the system over the barrier if the approach is close. Thus once the translational energy is sufficient to bring the BeF separation to that at the saddle point, the reaction proceeds with unit probability. There is no need to channel energy from one mode to another. The threshold is sharp. A higher energy trajectory is shown in Fig. 13. The behavior is typical: The trajectory passes over the barrier at its first possible opportunity, usually resulting in "cutting the cor-

ner"—passing to products through a configuration even more extended than that at the col.

These same trajectories suggest the explanation of the product energy distribution. For the Be + FH($v_1 = 0$) reaction at threshold the saddle point geometry results in vibrationally excited products. However, as energy increases the reactive trajectories which have been deflected over the barrier by collision with the repulsive wall now pass to products through configurations which

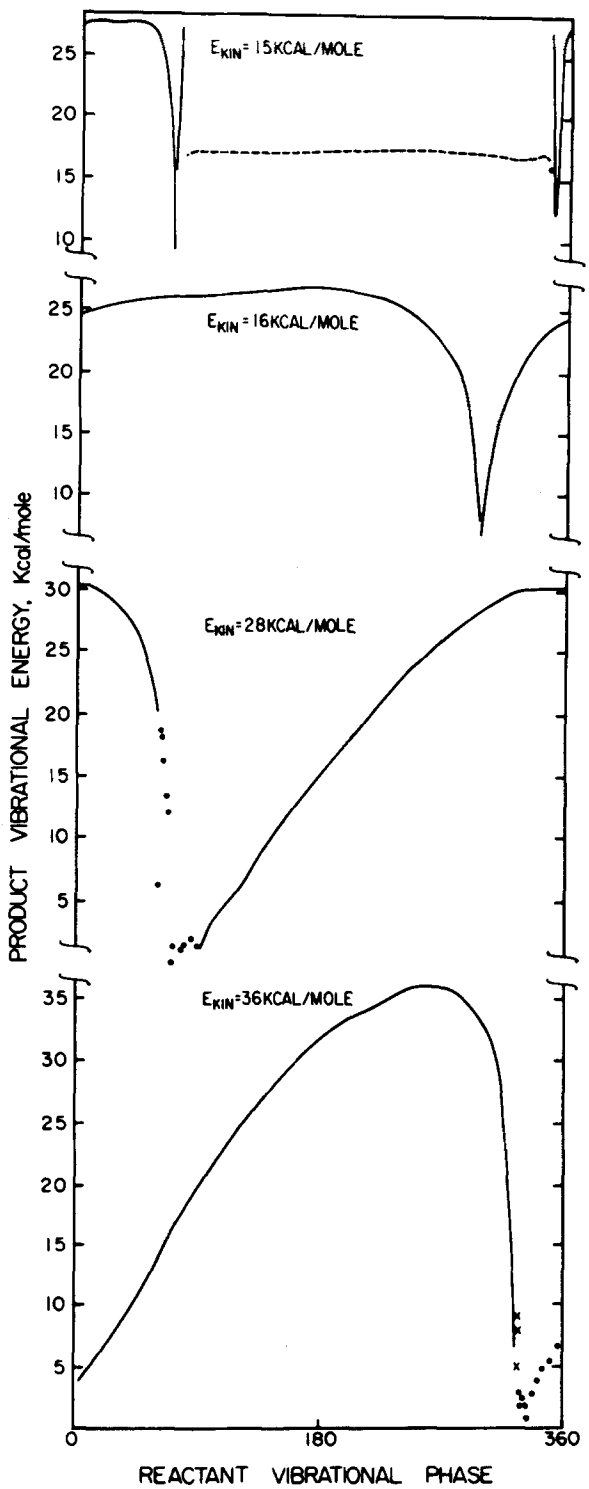

FIG. 8. The same as Fig. 7, except that the FH reactant was initially in its $v_1 = 1$ vibrational level.

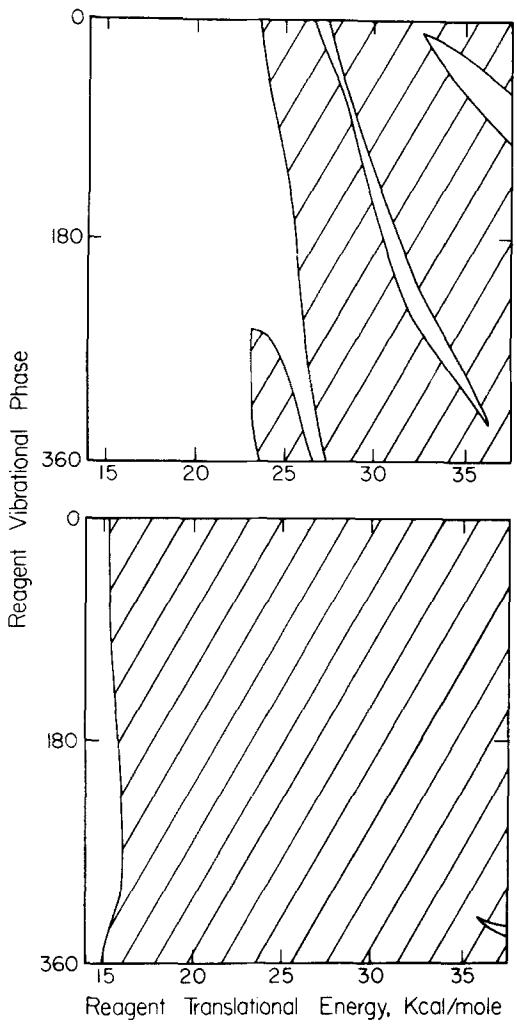

FIG. 9. Bands of reactive and nonreactive trajectories as a function of the initial translational energy and the initial vibrational phase for collinear Be + FH(v_1) on an *ab initio* potential surface. Shaded regions correspond to reactive trajectories. The upper panel shows FH initially in $v_1 = 0$ and the lower panel, $v_1 = 1$.

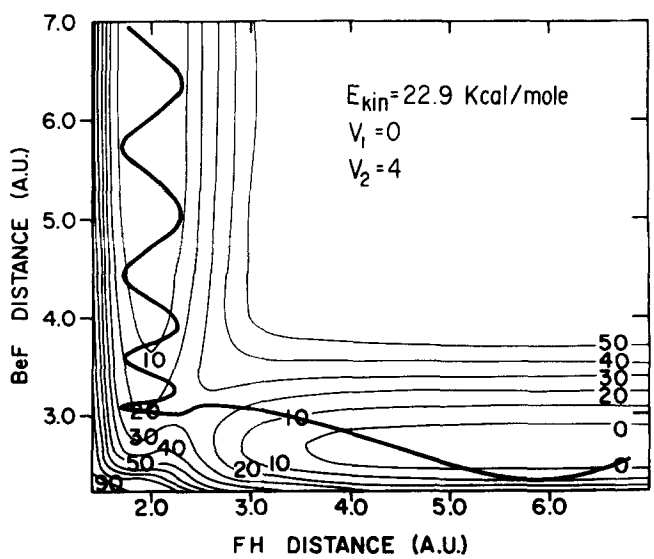

FIG. 10. A near threshold reactive trajectory for collinear Be + FH($v_1 = 0$) on the *ab initio* potential surface. Reactants enter from the upper left.

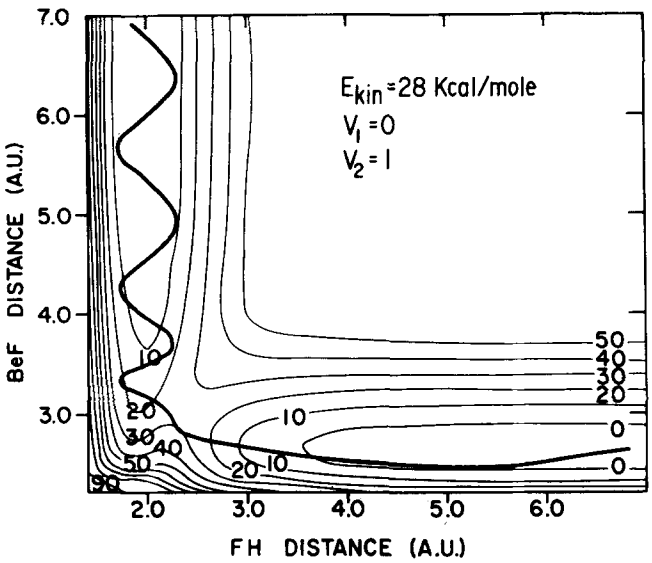

FIG. 11. A reactive trajectory for collinear Be + FH($v_1 = 0$) on the *ab initio* potential surface. The initial kinetic energy is about 5 kcal/mole above threshold. Reactants enter from the upper left.

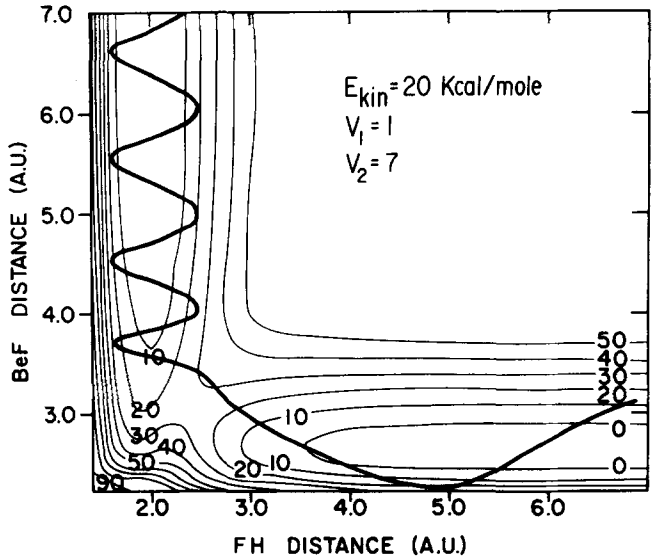

FIG. 13. A reactive trajectory for collinear Be + FH($v_1 = 1$) on the *ab initio* potential surface. The initial kinetic energy is a few kcal/mole above threshold. Reactants enter from the upper left.

are more compressed, and result in progressively decreased product vibration (compare Figs. 10 and 11). A high energy trajectory with initial translational energy of 36 kcal/mole is shown in Fig. 14. The trajectory passes high over the repulsive shoulder and results in vibrationally cold product.

Again, we contrast this behavior with the reaction involving vibrationally excited reactants. Here since most trajectories cut the corner, the final vibrational energy distribution is peaked towards higher values. Further, the weak dependence of these distributions on translational energy is understood: Increased translational energy, and hence increased total energy, permits the trajectories to cut the corner a little sooner, allowing slightly higher final vibrational energy, but the narrow pass prevents this from being a large effect. In addition, increased translation implies that some trajectories will penetrate to smaller BeF distances before the phase is right for passage over the barrier (see Fig. 15). Again a minor effect, it is this which broadens the product vibrational energy distribution.

The trajectories presented above were chosen to be typical of the system behavior. In general, we found that reactive trajectories sampled different parts of the potential energy surface depending on the initial vibrational state. However, it is interesting to look further at rather atypical trajectories, in order to determine the surface features which give rise to the reactive band

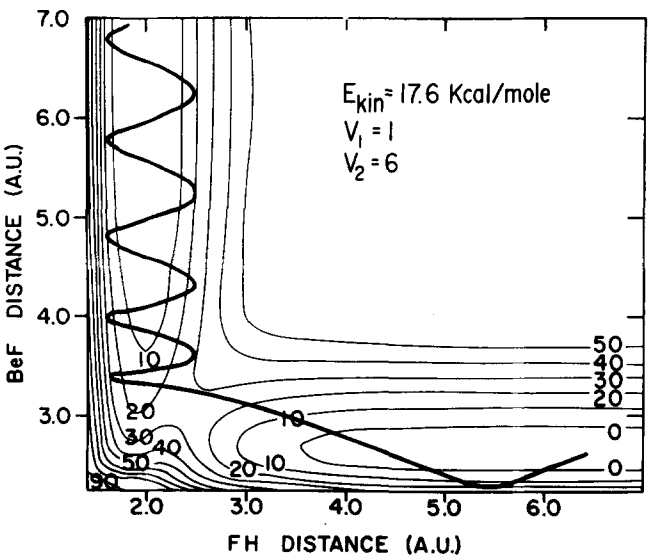

FIG. 12. A near threshold reactive trajectory for collinear Be + FH($v_1 = 1$) on the *ab initio* potential surface. Reactants enter from the upper left.

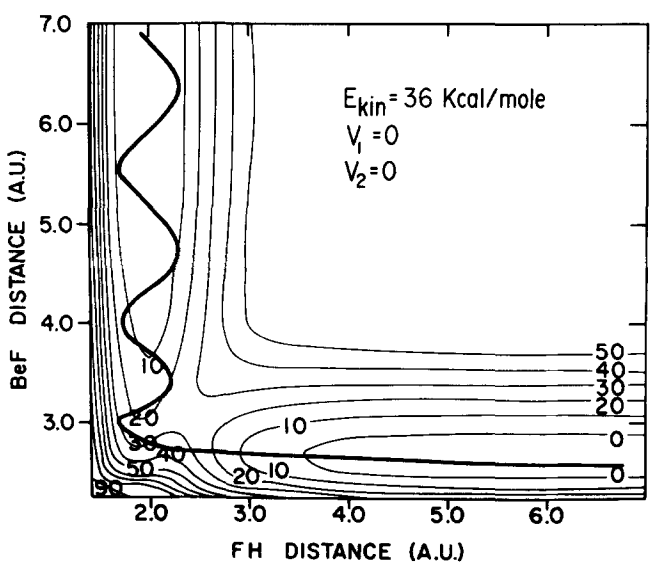

FIG. 14. A reactive trajectory for collinear Be + FH($v_1 = 0$) on the *ab initio* potential surface at a high initial kinetic energy. Reactants enter from the upper left.

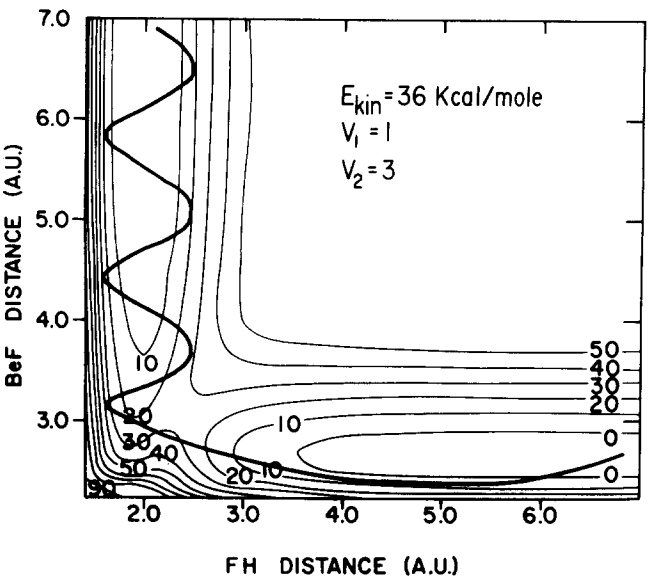

FIG. 15. A reactive trajectory for collinear Be + FH($v_1 = 1$) on the *ab initio* potential surface at a high initial kinetic energy. Reactants enter from the upper left.

structure. For the Be + FH($v_1 = 0$) system at lower energy it is seen that the edge of a reactive band is characterized by vibrationally excited products, and at higher energies that the final vibrational energy becomes a more complicated function of the initial phase. The cause of the former is clear: A slight shift in phase and a trajectory which is entering the product valley with its BeF distance increasing, and thus destined for high vibrational excitation, becomes one which is unreactive. This behavior is observed in other systems.[22] However, it is the behavior at higher energy which results from a special feature of this surface. As the translational energy increases, trajectories penetrate deeper into the corner of the potential energy surface. There a trajectory may be reflected at the shoulder, begin the return towards the entrance valley, but pass over the barrier on the return (see Fig. 16). Because such trajectories involve collision with a steep and sharply curved wall, it is clear that small asymptotic differences will be greatly amplified. Reflections with the repulsive wall have been cited as the cause of the statistical region in other systems,[22,27] but there is an interesting difference here. In the other systems it was mainly the mass combination which gave rise to sharp curvature and consequent reflection—in fact this effect can be seen with a simple hard wall potential[28]—while in this system it is the shape of the surface itself, and not a mass effect.

This corner also gives rise to the unreactive band which enters into both systems at higher translational energies. If the translational energy is sufficiently great, some of the trajectories will reach this part of the surface before the vibrational phase is appropriate for passage over the saddle point. There the repulsive forces may direct the trajectory straight back into the entrance valley.

IV. COMPARISON WITH LEPS

The dynamics of molecular collisions on LEPS and similar model potential energy surfaces has been studied in considerable detail. Systematic studies on particular reactive systems ($H + H_2$, $F + H_2$)[18,26] as well as general model systems[3] have led to a well documented body of information on the relationship between surface features and reaction dynamics. The appeal of LEPS, and of similar simple valence-bond type surfaces is that very few parameters other than well known aysmptotic structural constants are required to describe the entire surface. But this is a weakness also: While the LEPS equation has, in fact, been shown to give a remarkably good description of the $F + H_2$ system, there is no reason to expect that this will be so for all systems. Other empirical forms have been suggested, some for general use,[29] others specific,[30] but these have found little widespread application. For the large class of reactions which progress from essentially covalent bonding in the reactants to ionic bonding in the products, there is particular reason to suspect that the LEPS equation is inadequate.

To explore this problem, we have constructed a LEPS potential which reproduces insofar as is possible the shape of the *ab initio* Be + FH surface. The Morse parameters D_e, β, and r_e for each diatomic are taken from literature values. The exoergicity of the resulting surface is only 0.6 kcal/mole while that of the *ab initio* surface is 6 kcal/mole. However, in view of the high barrier it is felt that this difference is not significant for the energetic quantities discussed here. The adjustable parameters have been selected so that the barrier height and location are the same as on the *ab initio* surface. Relevant parameters are given in Table IV, and a collinear surface map shown in Fig. 17. Simply by examining the map, one can observe qualitative differences, differences which no adjustment of the LEPS

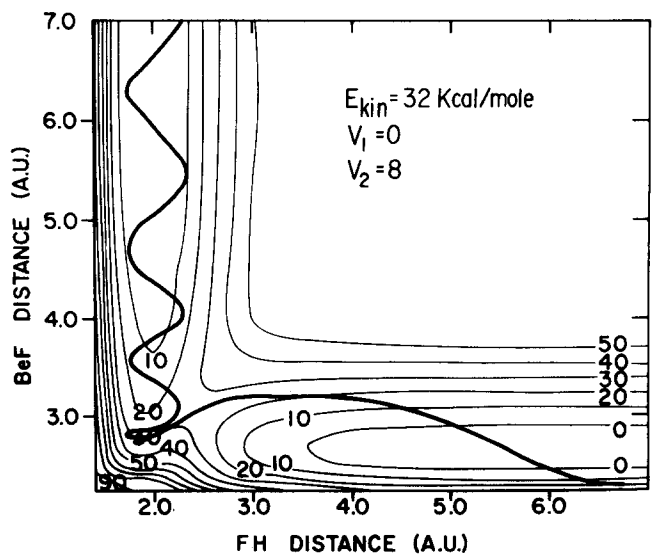

FIG. 16. A reactive trajectory for collinear Be + FH($v_1 = 0$) on the *ab initio* potential surface. Reactants enter from the upper left.

TABLE IV. Parameters used in LEPS potential surface.[a]

Parameter	HF	BeF	BeH
D_e, kcal/mole	138.3	138.8	56.6
R_e, a.u.	1.733	2.573	2.538
β, a.u.$^{-1}$	1.190	0.919	0.922
Sato parameter	−0.05	−0.06	−0.05

[a]See Ref. 3 for definition of parameters and functional dependence.

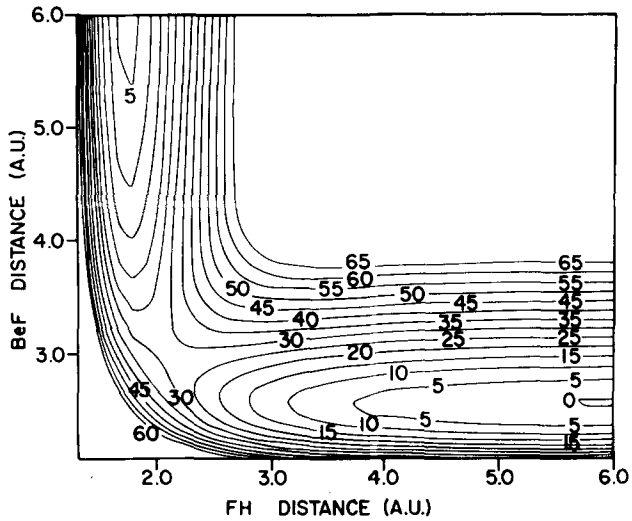

FIG. 17. Potential energy contours for collinear Be + FH from a LEPS model adjusted to have the same barrier position and height as the *ab initio* surface shown in Fig. 2. Contour units are kcal/mole.

parameters can eliminate. On both surfaces the saddle point is at a considerably extended geometry, but on the LEPS surface the reaction path curves quite gradually and smoothly over the barrier, while on the *ab initio* surface the curvature is much more abrupt. On both surfaces the saddle point is 28 kcal/mole above reactants, but on the LEPS surface the rise to this energy is gradual, while on the *ab initio* surface the last half of the rise occurs over a very short distance. The shape of the repulsive wall as it curves around the outside of the reaction path shows similar contrast.

These differences effect profound changes in the dynamics. Table V shows the probability of reaction as well as the average energy in product vibration as a function of initial translation for both Be + FH($v_1 = 0$) and Be + FH($v_1 = 1$). In each case the reaction threshold is somewhat above the *ab initio* result, reflecting less effective use of reactant vibration to surmount the barrier. Above threshold the contrast is more pronounced: The system reacts with unit probability over the whole range of energies studied, with an extremely sharp rise from threshold. The product vibrational energy distribution shows similar contrast. In the LEPS result the fraction of energy deposited in products remained essentially constant over the full range of energies, while in the *ab initio* result there was a sharp falloff with energy. The *ab initio* surface gave a much greater difference in the product vibrational energy depending on the reagent vibrational energy. The distributions of product vibrational energy, shown in Fig. 18 also show a weak energy dependence in contrast to the *ab initio* results. The contrast is particularly great for vibrationally cold reactants: For the LEPS surface the distributions are broad and peak at higher v_2 values, while for the *ab initio* surface, lower states are preferentially populated.

All of these results reflect the much smoother progress from reactants to products on the LEPS surface. On a more detailed level this can be seen in plots of the product vibrational energy as a function of the initial phase. Two such plots are shown in Fig. 19. Their general shape is typical of the entire range of energies studied. Because the system reacts with unit probability, there are no band edges representing transition between reactive and unreactive regions. However, in the case of the *ab initio* results it was seen that this function can have a complicated structure even with unit reaction probability. Nevertheless, with the LEPS surface the function is very smooth.

In summary, although the *ab initio* and LEPS surfaces have the same barrier height and location, the dynamics on the two surfaces is vastly different. In the *ab initio*

TABLE V. Probability of reaction and final vibrational energy for collinear Be + FH(v_1) on a LEPS surface.

$v_1 = 0$				$v_1 = 1$			
E_{kin}[a]	P_R	$\langle E_{v2}\rangle$[b]	%[c]	E_{kin}[a]	P_R	$\langle E_{v2}\rangle$[b]	%[c]
24.25	0.00	5.9[d]	...	18.25	0.00	17.2[d]	...
24.5	1.00	10.8	35	18.5	1.00	16.8	46
25.0	1.00	11.6	37	19.0	1.00	18.0	49
26.0	1.00	12.4	38	20.0	1.00	18.4	49
28.0	1.00	12.0	35	22.0	1.00	18.5	46
30.0	1.00	12.7	35	24.0	1.00	18.5	44
32.0	1.00	13.0	34	28.0	1.00	19.7	43
36.0	1.00	15.5	36	32.0	1.00	22.3	44
40.0	1.00	18.0	39	36.0	1.00	24.4	45
				40.0	1.00	28.4	49

[a]Reactant kinetic energy in kcal/mole.
[b]Average product vibrational energy in kcal/mole.
[c]Percent of available energy ($E_{kin} + E_{v_1} + \Delta E$) in product vibration.
[d]Average final vibrational energy in unreacted FH molecule.

results, reagent translation and vibration is only weakly coupled until the close interaction region is reached. There results quite specific use of energy in the reactants, and disposal of energy in the products. The LEPS surface evolves much more smoothly from the entrance to the exit channels, causing effective mixing of reactant translation and vibration and much less specific energy disposal.

V. SUMMARY

A potential energy surface for the collinear chemical reaction Be + FH → BeF + H has been calculated using *ab initio* quantum mechanical techniques. While the reaction occurs on a single adiabatic potential energy surface, the electronic configurations appropriate to separate reactants and products are quite different, the bonding in reactants essentially covalent, and the bonding in products essentially ionic. A number of levels of basis set approximation were explored, seeking a basis set which described reactants and products at an equivalent and acceptable level.

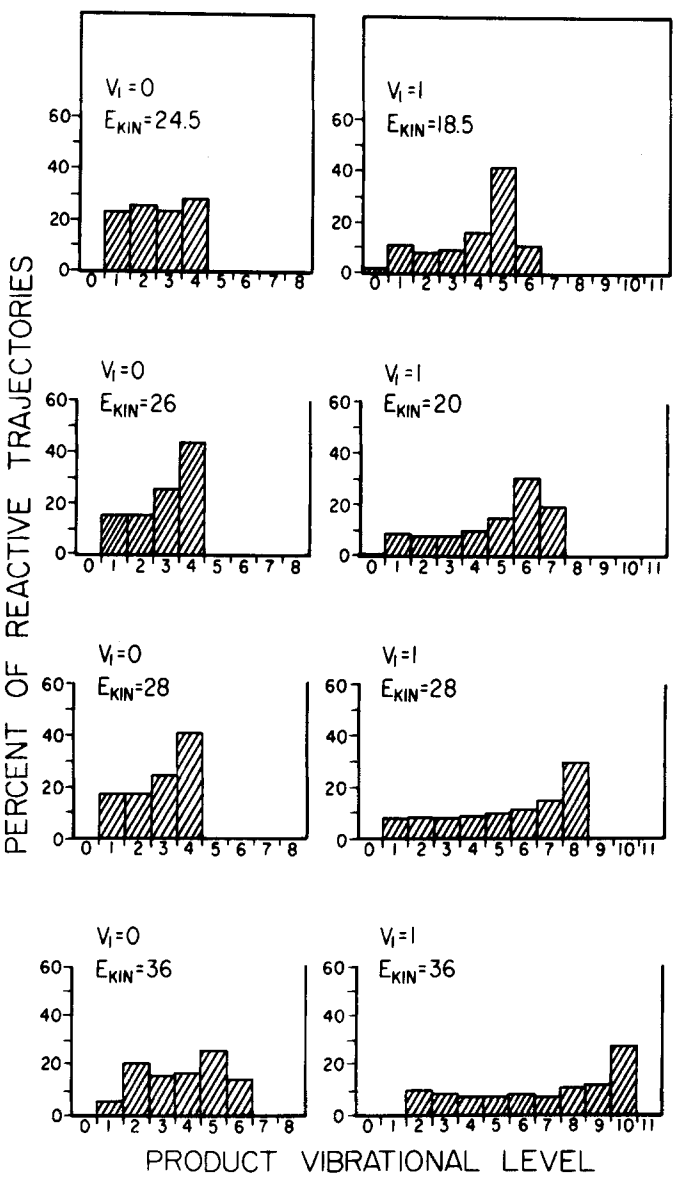

FIG. 18. Distribution among final vibrational levels for Be + FH → BeF + H for selected initial translational energies (in kcal/mole) and initial vibrational levels $v_1 = 0$ and $v_1 = 1$. Results were obtained from collinear classical trajectory calculations on a LEPS potential surface.

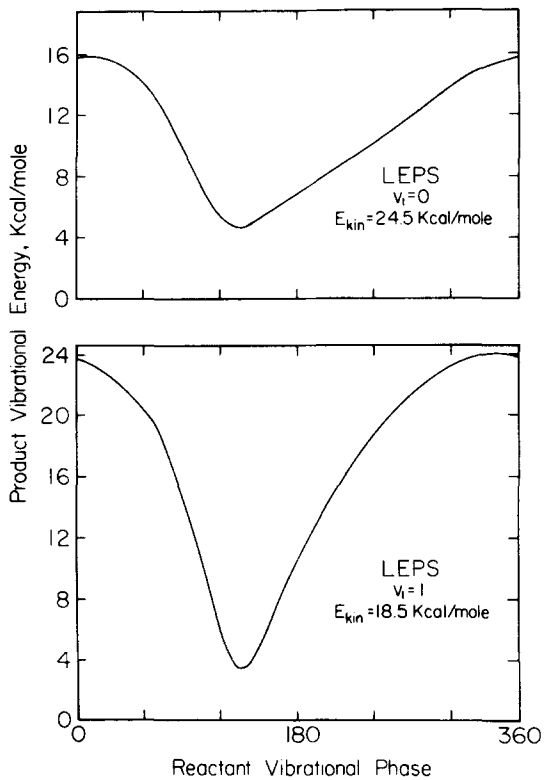

FIG. 19. Product vibrational energy as a function of reactant vibrational phase from classical trajectory calculations on a LEPS potential surface for collinear Be + FH → BeF + H. Results are shown for initial translational energies somewhat above threshold and initial vibrational levels $v_1 = 0$ and $v_1 = 1$. The unit reaction probability and smooth behavior as a function of initial phase shown here are typical of all the results on the LEPS surface and should be contrasted with the results on an *ab initio* surface shown in Figs. 7 and 8.

Preliminary studies demonstrated that a minimum basis set complete CI calculation was not acceptable, as it failed to yield stable products. Addition of a $2p$ function to the Be atom, with reoptimization of the orbital exponents, gave an improved, but still inadequate result. A larger basis set made a complete CI approach impractical. Thus the CI was performed with orbitals obtained using the iterative natural orbital method of Bender and Davidson,[8] with configurations selected according to the first order wavefunction scheme developed by Schaefer.[9] The configurations retained were chosen so that the same kind of excitations were included in the two asymptotic ground state configurations. The resulting calculation is not expected to give quantitative accuracy. However, it represents a reasonable compromise between accuracy and economy. Further, because of the effort to describe the asymptotic channels at an equivalent level, it should give reasonably good results for the energy differences which comprise the potential energy surface.

Visual inspection of the resulting surface showed it to be quite different in character from the well known

$H + H_2$ and $F + H_2$ surfaces. The curvature of the reaction path is much more abrupt, the atom in both entrance and exit valleys effecting little distortion of the molecule until the approach is quite close. The saddle point is 28 kcal/mole above reactants, and occurs at a geometry where both internuclear separations are extended about 0.4 bohr from their asymptotic equilibrium values. There being no simple analytic function available to fit such a surface, a bicubic spline function was used to obtain a piecewise fit to the calculated points.

The quasiclassical trajectory method was used to study the dynamics of the Be + FH(v_1) → BeF(v_2) + H reaction for $v_1 = 0$ and $v_1 = 1$ over a range of relative translational energies. All aspects of the results showed that the additional vibrational energy had a profound effect on the dynamics. For the vibrationally cold reaction ($v_1 = 0$), the reaction probability rises from the threshold energy, peaking about 4 kcal/mole above threshold at a value below unity, and falls slowly thereafter. The product energy distribution shows a strong translational energy dependence, with the average fraction of energy as product vibration very low at intermediate and higher total energies. With vibrationally excited reactants ($v_1 = 1$), the probability of reaction rises more steeply from threshold, is unity over a wide energy range, and falls only slightly at higher energy. The product vibrational energy distributions are broader and less energy sensitive. Examination of representative trajectories makes it possible to identify the surface features which give rise to this behavior. Vibration and translation couple only weakly in the entrance valley, so that the reactant vibrational energy is very important in the way in which the barrier is crossed. Trajectories for the cold and hot reactants pass over the barrier in quite different areas of the surface on the average, leading to the specificity in the product energy disposal.

A LEPS surface was constructed to have the same barrier height and position. The overall appearance was qualitatively different, and this difference was reflected in differences in the dynamics. The reaction path was more gently curved, resulting in better coupling of reactant translation and vibration, with less specific energy use and disposal. This is an important result, for it underscores the need to broaden the usual picture of simple triatomic A + BC reactions. While studies on LEPS functions have led to useful generalizations on energy use and deposition for systems like $H + H_2$ and $F + H_2$, reactions which involve quite different configurations in the asymptotic channels have quite different topological features and dynamics.

As indicated in the Introduction, this study was originally motivated by experimental results for Ba + FH,[4] and similar experimental results have subsequently been obtained in reactions of Sr and Ca.[5] In concluding, we will consider what, if anything, the present study can tell us about these systems. The most striking fact is that the present results for Be + FH are quite similar to the experimental results in terms of energy specificity and energy disposal. This behavior has been traced to the non-LEPS appearance of the potential energy surface here, and that, in turn, reflects the rather sudden change in electronic configuration in passing from reactants to products. While it is tempting to postulate that the surfaces for the other alkaline earths with FH may be similar to that for Be + FH, we really have no basis for such a conclusion. A more reasonable statement is that these surfaces also differ greatly from the LEPS model, probably because they too undergo a sudden change in electronic structure, due, perhaps, to an electron jump, on passing from reactants to products.

One final point which must be considered in any comparison of the present work with experiment is the fact that restriction to collinear geometry is a rather severe approximation to the true, three-dimensional dynamics. It is by far the most severe approximation made in the present study of Be + FH, and in future studies it would be most desirable to relax this constraint. The present study is not intended to imply that the collinear approach is favored. Indeed for the Li + HF system, an *ab initio* calculation[31] showed a preference for a highly bent minimum energy path. Nevertheless, the present study demonstrates important differences between LEPS and *ab initio* surfaces for determining reaction dynamics.

[1]For recent reviews see (a) J. L. Kinsey, Ann. Rev. Phys. Chem. **28**, 349 (1977); (b) R. D. Levine and R. B. Bernstein, *Molecular Reaction Dynamics* (Oxford University, New York, 1974).

[2]Recent reviews include (a) R. N. Porter and L. M. Raff in *Dynamics of Molecular Collisions, Part B*, edited by W. H. Miller (Plenum, New York, 1976), p. 1; (b) P. J. Kuntz, *ibid.*, p. 53; (c) R. N. Porter, Ann. Rev. Phys. Chem. **25**, 317 (1974).

[3]P. J. Kuntz, E. M. Nemeth, J. C. Polanyi, S. D. Rosner, and C. E. Young, J. Chem. Phys. **44**, 1168 (1966); J. C. Polanyi and W. H. Wong, *ibid.* **51**, 1439 (1969); M. H. Mok and J. C. Polanyi, *ibid.* **51**, 1451 (1969).

[4]J. G. Pruett and R. N. Zare, J. Chem. Phys. **64**, 1774 (1976).

[5]Z. Karny and R. N. Zare, J. Chem. Phys. **68**, 3360 (1978).

[6]Recent reviews include (a) H. F. Schaefer, *The Electronic Structure of Atoms and Molecules* (Addison–Wesley, Reading, MA, 1972); (b) *Methods of Electronic Structure Theory*, edited by H. F. Schaefer (Plenum, New York, 1976).

[7]P.-O. Löwdin, Phys. Rev. **97**, 1474 (1955); see also Ref. 6.

[8]C. F. Bender and E. R. Davidson, J. Phys. Chem. **70**, 2675 (1966); see also Ref. 6.

[9]See Reference 6.

[10]G. Das and A. C. Wahl, J. Chem. Phys. **47**, 2934 (1967); see also Ref. 6.

[11]W. A. Goddard, Phys. Rev. **157**, 73, 81, 93 (1967); see also Ref. 6.

[12]F. O. Ellison, J. Am. Chem. Soc. **85**, 3540 (1963); P. J. Kuntz and A. C. Roach, J. Chem. Soc. Faraday Trans. II **68**, 259 (1972); J. C. Tully, J. Chem. Phys. **58**, 1396 (1973).

[13]N. Sathyamurthy, J. W. Duff, C. Stroud, and L. M. Raff, J. Chem. Phys. **67**, 3563 (1977).

[14]N. Sathyamurthy and L. M. Raff, J. Chem. Phys. **63**, 464 (1975).

[15]International Mathematics and Statistics Library. See also J. H. Ahlberg, E. N. Nilson, and J. L. Walsh, *The Theory of Splines and Their Application* (Academic, New York, 1967).

[16]J. T. Muckerman, J. Chem. Phys. **54**, 1155 (1970); J. R. Krenos, R. K. Preston, R. Wolfgang, and J. C. Tully, *ibid.* **60**, 1634 (1974).

[17]G. C. Schatz, J. T. Bowman, and A. Kupperman, J. Chem. Phys. **63**, 685 (1975); G. C. Schatz and A. Kupperman, *ibid.* **65**, 4668 (1976).

[18]M. Karplus, R. N. Porter, and R. D. Sharma, J. Chem. Phys. **43**, 3259 (1965); D. L. Bunker, Methods Comput. Phys. **10**, 287 (1971); see also Ref. 2(a).
[19]V. B. Cheng, H. H. Suzukawa, and M. Wolfsberg, J. Chem. Phys. **59**, 3992 (1973).
[20]C. C. Rankin and W. H. Miller, J. Chem. Phys. **55**, 3150 (1971).
[21]W. H. Miller and T. F. George, J. Chem. Phys. **56**, 5668 (1972).
[22]J. S. Wright, K. G. Tan, and K. J. Laidler, J. Chem. Phys. **64**, 970 (1976).
[23]H. Schor, Ph.D. thesis, Columbia University, 1978.
[24]R. E. Howard, A. C. Yates, and W. A. Lester, J. Chem. Phys. **66**, 1960 (1977).
[25]R. N. Porter and M. Karplus, J. Chem. Phys. **40**, 1105 (1964); P. Siegbahn and B. Liu, J. Chem. Phys. **68**, 2457 (1978).
[26]J. T. Muckerman, J. Chem. Phys. **56**, 2997 (1972); C. F. Bender, S. V. O'Neil, P. K. Pearson, and H. F. Schaefer, *ibid.* **56**, 4626 (1972).
[27]J. W. Duff and D. G. Truhlar, Chem. Phys. **4**, 1 (1974); F. Schnabel and S. Chapman, Chem. Phys. Lett. **57**, 189 (1978).
[28]R. A. LaBudde, P. J. Kuntz, R. B. Bernstein, and R. D. Levine, J. Chem. Phys. **59**, 6286 (1973).
[29]D. L. Bunker and C. A. Parr, J. Chem. Phys. **52**, 5700 (1970).
[30]P. J. Kuntz, E. M. Nemeth, and J. C. Polanyi, J. Chem. Phys. **50**, 4607 (1969).
[31]G. G. Balint-Kurti and R. N. Yardley, Faraday Discuss. Chem. Soc. **62**, 77 (1977).